*Defect and Diffusion Forum*
*ISSN: 1662-9507, Vol. 450, pp 127-137*
*doi:10.4028/p-TB3Cbv*

*Submitted: 2026-01-28*
*Revised: 2026-02-24*
*Accepted: 2026-02-25*
*Online: 2026-04-15*

# Towards Solid-State Recycling of Ti6Al4V: Defining a Sustainable Machining Process Window for Low-Oxidation Chips

ORTIZ-DE-ZARATE Gorka[1,a,*], RODRÍGUEZ Iñigo[1,b], ORUNA Ainara[1,c], OTALORA Harry[1,d], ETXEBESTE Mikel[1,e], and ARRAZOLA Pedro J.[1,f]

[1]Mondragon Unibertsitatea, Faculty of Engineering, Loramendi 4, Arrasate-Mondragón, 20500, Spain

[a]gortizdezarate@mondragon.edu, [b]irodriguez@mondragon.edu, [c]ainara.oruna@alumni.mondragon.edu, [d]hyotalora@mondragon.edu, [e]metxebeste@mondragon.edu, [f]pjarrazola@mondragon.edu (*corresponding author)

**Keywords:** Recycling; Oil-free machining; Sub-zero cooling; Titanium

**Abstract.** Titanium is a Critical Raw Material for the European aerospace sector, yet its manufacturing is characterized by high buy-to-fly ratios and significant waste in the form of chips. Solid-state recycling (SSR) presents a low-energy alternative to remelting for chip revalorisation. However, its viability is strictly limited by chip oxidation. This study investigates the influence of milling parameters (cutting speed and radial depth of cut), and coolants (emulsion, $LCO_2$ and dry), on cutting forces and chip quality (morphology and oxidation) to define a process window for generating low oxidation chips, enabling further SSR routes. By correlating cutting forces with chip analysis, the results reveal that emulsion cooling yields chips with the lowest oxidation, despite potential oil contamination of the feedstock. While $LCO_2$ effectively reduces oxidation at lower material removal rates, high thermal loads overwhelm its cooling capacity, resulting in oxidation comparable to dry cutting. These findings establish the machining parameters necessary to produce high-quality, recyclable feedstock, bridging the gap between subtractive manufacturing and circular material flows.

## Introduction

Titanium holds great importance for the European Union's (EU) industrial sectors, primarily due to its high strength-to-weight ratio, superior corrosion resistance, and biocompatibility properties. However, the EU's position within the global titanium value chain presents significant strategic vulnerabilities. As a net importer of titanium products with an import-to-export ratio of 2:1, the EU relies heavily on external suppliers [1]. Critically, the region lacks both domestic reserves of titanium ore and sponge production infrastructure, creating a dependency on supply chains dominated by geopolitically sensitive regions. Due to these vulnerabilities, the European Commission designated titanium metal as a Critical Raw Material in 2020 [2].

The aerospace sector dominates European consumption, accounting for 67% of all titanium products, with Ti6Al4V being the primary alloy [3]. Future demand pressures will intensify this challenge; according to global market forecasts, approximately 43,420 new aircraft are anticipated over the next two decades to accommodate a 3.6% annual growth in passenger traffic, as seen in Figure 1 [4]. This trajectory suggests a dramatic increase in titanium demand precisely when supply security remains uncertain.

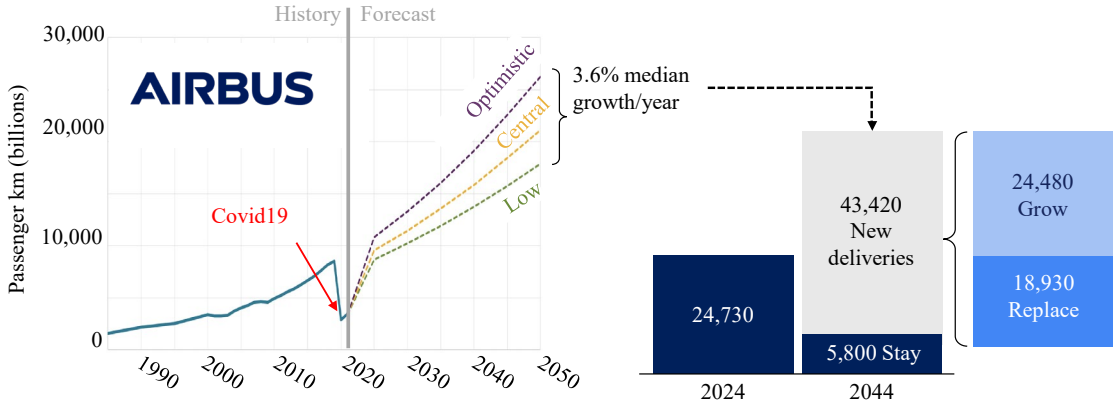


**Fig. 1.** Forecast of air traffic and aircraft delivery by Airbus [4].

Current manufacturing practices further undermine resource efficiency. Aeronautical machining commonly exhibits buy-to-fly ratios of 9:1 or higher, meaning nearly 90% of the material becomes chips [5]. Although these chips retain the thermomechanical properties of the virgin alloy, they are typically exported or recycled via conventional remelting [1]. Despite lower energy demand compared to primary production, remelting remains energy-intensive and entails material losses through oxidation and dross formation.

Solid-state recycling (SSR) offers a viable alternative by consolidating chips without melting, thereby reducing energy consumption and promoting circularity within the EU [6]. However, industrial deployment is constrained by process stability and, critically, chip quality—particularly morphology and oxidation state. In Ti6Al4V SSR, chip morphology, surface cleanliness, and interstitial content (O, N, C) govern consolidation success [7] and compliance with aeronautical specifications [8].

The machining of Ti6Al4V presents inherent challenges due to its high-temperature strength and low thermal conductivity. Tool-chip interface temperatures often exceed 800–1000°C, promoting surface oxidation [9]. These oxides embrittle chips [10], reducing ductility and compromising SSR feedstock quality. Therefore, minimizing oxygen uptake during machining is essential for SSR viability [11].

Recent research has established that oxygen is not merely a passive environmental factor but an active process variable. Controlling it can alter chip formation mechanisms and tribological conditions [12]. Machining under oxygen-free atmospheres reduces cutting forces, tool wear, and subsurface deformation by suppressing tribo-oxidation [13–16], thereby enhancing chip suitability for SSR. However, fully inert chambers are impractical for industrial implementation.

Liquefied carbon dioxide ($LCO_2$) cooling represents a scalable alternative. It significantly lowers cutting temperatures [17], reduces tool wear [18], and avoids oil contamination associated with emulsions [19]. By delivering localized sub-zero cooling, $LCO_2$ mitigates oxidation-driven degradation and may bridge the gap between conventional and inert machining.

Despite these advances, no study has systematically quantified the combined effect of milling parameters and cooling strategies to define an operational window for producing low-oxidation, SSR-ready chips. This work addresses that gap by evaluating the influence of machining parameters and cooling/lubrication conditions on chip oxidation. Process forces are monitored as a proxy for deformation energy, and chip quality is assessed via macroscopic oxidation indicators to identify parameter sets that minimize oxygen uptake. This research aims to provide a validated guideline for transforming titanium machining waste into a valuable resource for circular manufacturing.

## Methodology

*Experimental plan and procedure*

A parametric study was conducted to define the machining process window. Cutting speed ($V_c$) was varied from 40 to 240 m/min, while the radial depth of cut ($a_e$) ranged between 0.5 and 1 mm. Cutting speed primarily governs cutting temperature, while radial depth of cut influences chip

thickness and thus the rate of heat evacuation through the Ti6Al4V chips. Cooling and lubrication conditions were also modified, comparing conventional emulsion cooling with liquid carbon dioxide ($LCO_2$)-assisted and dry machining (Figure 2a).

All remaining machining parameters, such as the feed per tooth ($f_z$) and the axial depth of cut ($a_p$), were kept constant at 0.1 mm/tooth and 15 mm, respectively. Each condition was repeated three times to assess experimental variability. The combinations of highest $V_c$ and $a_e$ were not tested under $LCO_2$ and dry conditions due to the risk of tool failure caused by excessive thermomechanical loads.

Analysed output parameters for defining a sustainable machining process window for low-oxidation chips were: (i) cutting forces, (ii) chip oxide colour, and (iii) chip microstructure (Figure 2a). Cutting forces were recorded during machining, and chips were collected ex-situ in a dedicated clean container to avoid cross-contamination. Chip oxidation was qualitatively assessed via colour using a Leica DMS 1000 microscope at ×5 magnification. This evaluation followed established literature correlations [13] linking oxide layer composition and thickness to optical appearance.

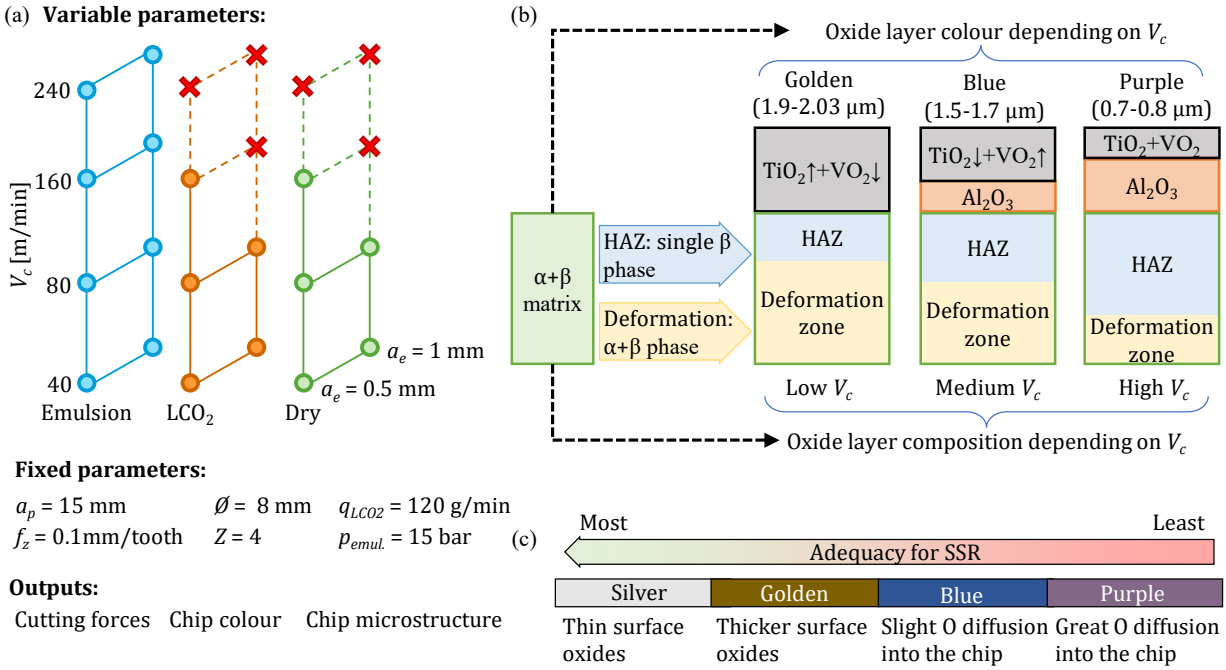


**Fig. 2.** (a) Experimental conditions and monitored outputs; (b) Chip oxide layer colour according to the oxide layer composition, adapted from [20]; (c) Colour grading of the chips selected for the study.

According to Keren et al. [20], chip colour reflects the oxide stratification and thermal history (Figure 2b). At lower cutting temperatures, chips exhibit a yellow/golden appearance, associated with a relatively thick single-layer $TiO_2$+$VO_2$ scale (~2 µm), with colour dominated by $TiO_2$. At higher temperatures (>1000 °C), a bilayer oxide forms, consisting of an inner $Al_2O_3$ layer and an outer $TiO_2$+$VO_2$ layer (~1.5–1.7 µm), leading to a blue coloration driven by both $VO_2$ formation and optical interference.

Under the highest thermal loads, the total oxide thickness decreases: the outer $TiO_2$+$VO_2$ layer thins to ~700–800 nm, while the inner $Al_2O_3$ layer grows. This outer-layer thickness promotes constructive interference in the violet range, resulting in a purple appearance. The formation of an inner $Al_2O_3$ layer indicates a high-temperature oxidation regime in which Ti- and V-rich oxides have already formed and Al is subsequently driven to react. This condition correlates with enhanced oxygen diffusion beneath the oxide scale into the titanium matrix [21]. Therefore, the observed colour evolution serves as a direct indicator of oxide chemistry, peak cutting temperature, and the extent of the underlying heat-affected zone (HAZ), and consequently reflects its suitability for SSR (Figure 2c).

After classifying the chips produced under the different cutting conditions according to their oxidation colour, representative samples were selected for microstructural examination of both the free and back surfaces of the chip (Figure 3a). The microstructure was analysed on polished cross sections that were subsequently chemically etched using Kroll's reagent (100 mL $H_2O$, 3.5 mL HF, and 7 mL $HNO_3$). This preparation enabled clear observation of the free surface (where the characteristic saw-tooth morphology associated with adiabatic shear banding develops) as well as the back surface (Figure 3b). The back surface is of particular interest because it slides along the tool rake face and is subjected to high contact pressures and severe shear stresses [22]. Consequently, the influence of cutting temperature on the chip microstructure is expected to be most pronounced in this region, primarily through thermally driven phase transformations [23].

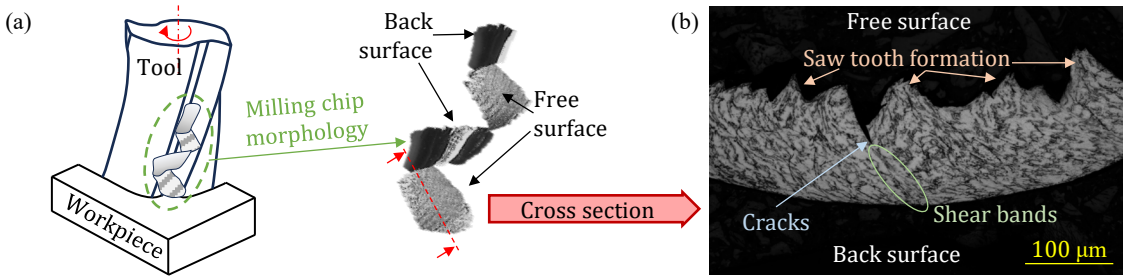


**Fig. 3.** Microstructure analysis of the formed chips: (a) Detail of chip free and back surface; (b) Example of a chip cross-section microstructure and most relevant features.

*Experimental setup*

Machining tests were performed on a LAGUN GVC 1000-HS machining centre equipped with through-spindle $LCO_2$ delivery. A four-flute end mill (Gühring 60818.000) with four 0.5 mm internal cooling channels was mounted in a shrink-fit tool holder (Figure 4a). The $LCO_2$ flow rate ($q_{LCO2}$) was set to 120 g/min, while emulsion coolant ($p_{emul.}$), when used, was supplied externally at 15 bar. Ti6Al4V workpiece was mounted on a Kistler 9139AA dynamometer (Figure 4b), and cutting forces were acquired at 10 kHz over a machined length of 105 mm to ensure steady-state.

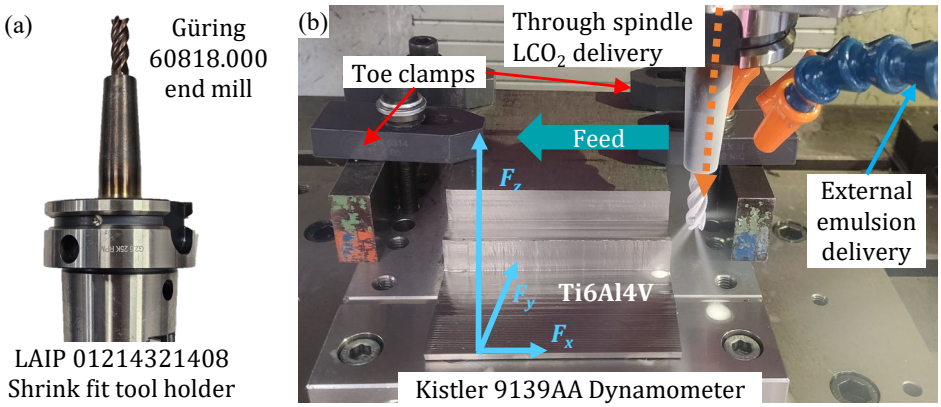


**Fig. 4.** (a) End mill and tool holder employed; (b) Experimental setup for force acquisition.

The trigger for cutting force signal acquisition was synchronised with the machine-tool axis movements in order to minimise the time that the $LCO_2$ jets were impinging on the Kistler dynamometer, and to make this time consistent across experiments. Controlling this was important as the $LCO_2$ can cool the dynamometer and create thermal contractions on the piezoelectrics, creating signal drift, if the jets impinge for too long on the sensor. The acquired force signals were subsequently processed using a dedicated MATLAB script. A low pass filter was applied at 10% of the natural frequency of the experimental setup (1500 Hz) and the region of the signal that corresponded to the cutting process was detected via up and down flanks. The selected representative force values for comparison between experimental conditions were the maximum filtered values of the stable region of the signal, as shown in Figure 5.

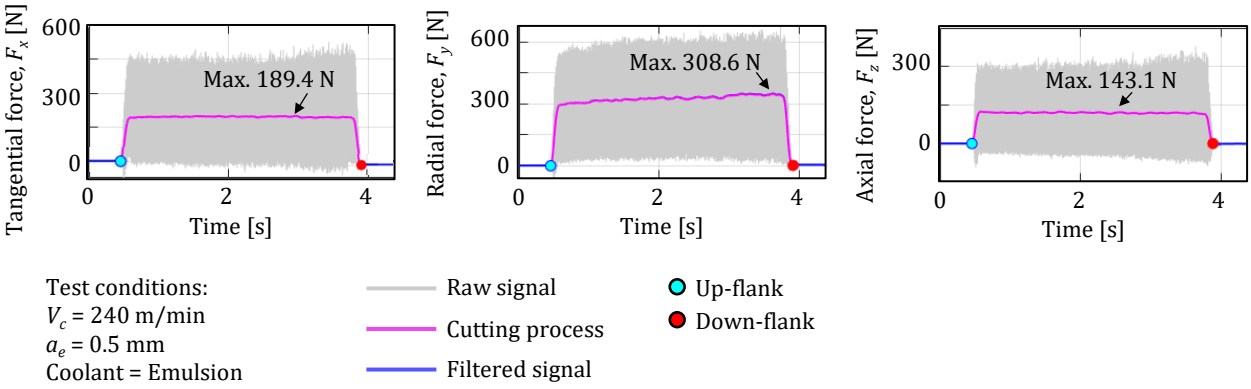


**Fig. 5.** Processing of the force signals, detection of the cutting region and representative values.

## Results and Discussion

*Cutting forces*

The evolution of cutting force components for each experimental condition is presented in Figure 6. The analysis focuses primarily on the tangential ($F_x$) and radial ($F_y$) forces. The axial component ($F_z$) was found to be negligible, as the side milling operation at low radial immersions ($a_e$ < 25% of tool radius) generates minimal vertical loading, and the tested variables showed no significant influence on this direction (Figure 6c).

At low radial depth of cut ($a_e$ = 0.5 mm), no significant differences were observed between cooling strategies. However, a slight decreasing trend in the tangential component ($F_x$) is evident as cutting speed ($V_c$) increases. This phenomenon is characteristic of titanium alloys and is attributed to thermal softening within the primary shear zone. As cutting speed increases, the adiabatic temperature rise reduces the yield strength of the material, thereby lowering the specific cutting energy required for chip formation [23].

In contrast, at the higher radial depth of cut ($a_e$ = 1.0 mm), the influence of the cooling strategy becomes pronounced. Radial forces ($F_y$) increased substantially across all conditions due to the larger engagement angle and chip load (Figure 6b). Notably, with regard to the tangential component, both $LCO_2$ and dry conditions generated significantly higher forces than emulsion. This disparity is attributed to the superior tribological performance of the emulsion; its lubricating effect reduces the friction coefficient at the tool-chip interface. Conversely, the lack of lubrication in $LCO_2$ and dry environments promotes higher temperatures and, potentially, adhesion of the workpiece material to the rake face [24].

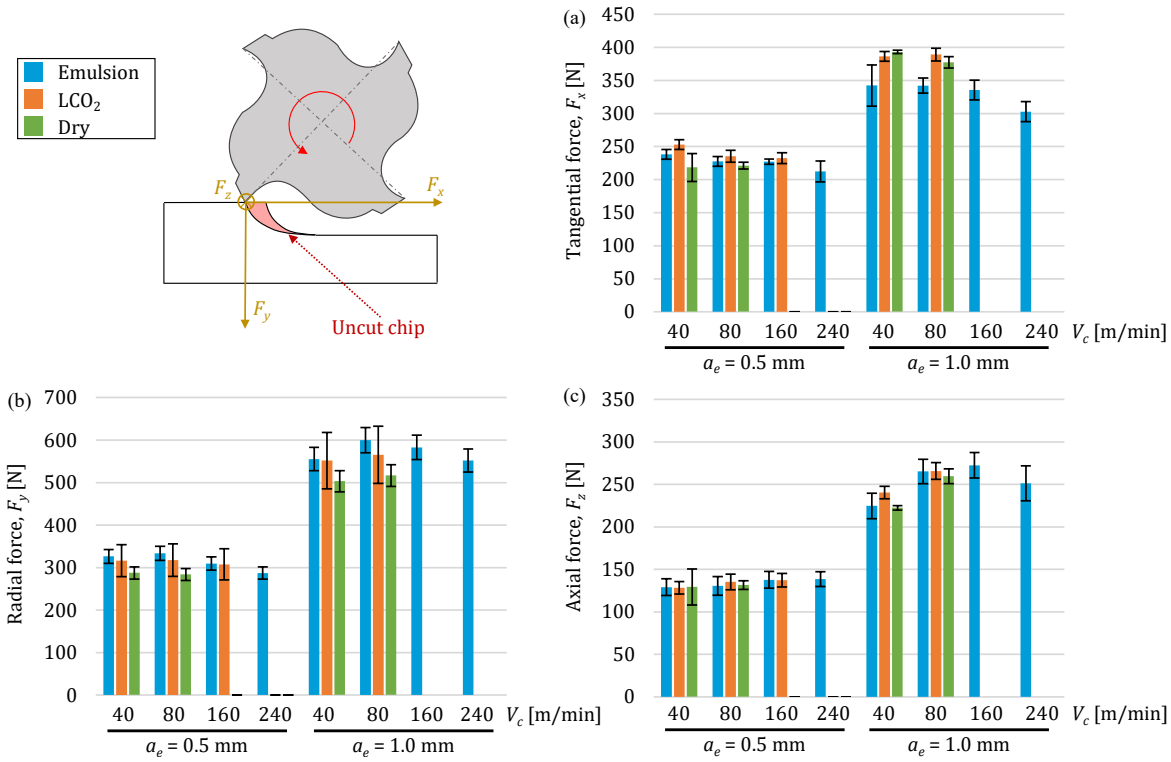


**Fig. 6.** Cutting forces results: (a) Tangential forces; (b) Radial forces; (c) Axial forces.

*Chip macroscopic analysis – Oxide colour*

Following the oxide colour grading methodology described in Figure 2b and c, a qualitative comparison was performed by examining the oxide colours of chips produced under the different machining parameter sets. As shown in Figure 7, chips generated at low radial depth of cut values ($a_e$ = 0.5 mm) exhibit more regular and well-defined morphology, whereas those produced at higher $a_e$ values display irregular shapes and chip agglomeration under $LCO_2$-assisted and dry machining conditions. This behaviour can be attributed to the higher cutting temperatures associated with these conditions compared to emulsion-cooled machining. Increased friction at the tool–chip interface may have hindered stable shearing of the Ti6Al4V material and promoted local adhesion, leading to partial welding of the chips.

Notably, cutting speed ($V_c$) had the greatest effect at high radial depths of cut in both $LCO_2$-assisted and dry cutting, whereas emulsion cooling consistently produced stable, low-oxidation chips, even under severe machining conditions.

Among the investigated strategies, emulsion cooling proved to be the most effective in mitigating chip oxidation due to a combined effect of tribological, physical, and thermal mechanisms. Firstly, the superior lubricity of the emulsion reduced tool–chip friction, thereby lowering heat generation at the source. Secondly, the continuous flood physically shielded the freshly formed chip surfaces from atmospheric oxygen. Finally, regarding thermal management, although $LCO_2$ reaches significantly lower temperatures (-78°C) via the sublimation of dry ice particles, its heat removal capability is limited by the low thermal conductivity of the gas phase and the brief contact time at the interface. In contrast, the liquid emulsion acts as a more efficient thermal sink, utilising the high heat capacity and convective heat transfer of the water-oil mixture to extract heat more effectively, as demonstrated by Pušavec et al. [25]. This superior cooling efficiency reduced the thermal load on the chips compared to $LCO_2$ or dry machining.

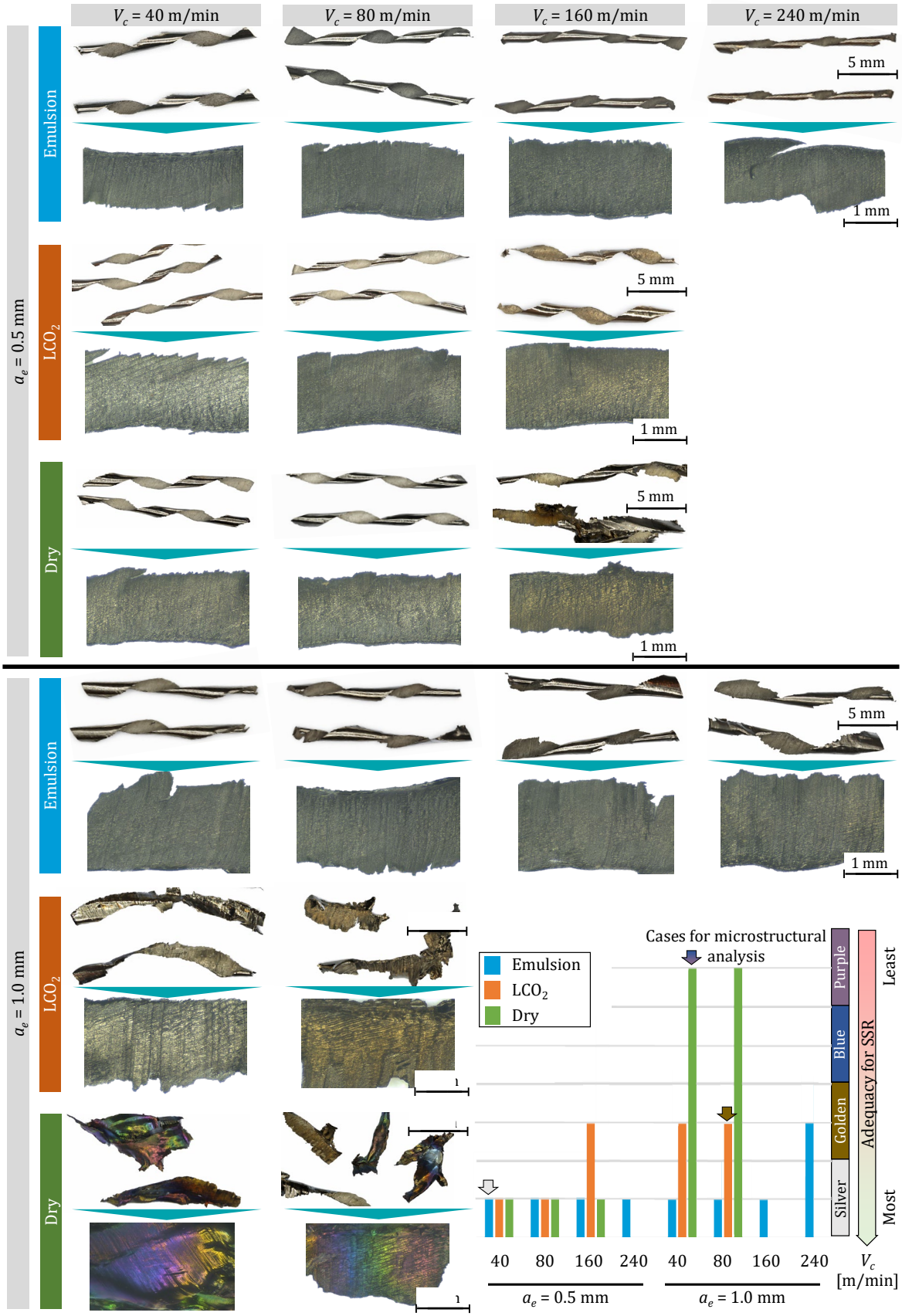


**Fig. 7.** Macroscopic chip analysis and qualitative oxide colours comparison along cutting conditions.

As illustrated in the bar chart in Figure 7, oxide colours associated with a significant development of an inner $Al_2O_3$ layer were predominantly observed under dry and $LCO_2$-assisted machining

conditions, particularly at high cutting speeds or large radial depths of cut. These oxide states are considered potentially the most brittle and therefore the most detrimental for SSR routes [20].

*Chip microstructure analysis*

After the macroscopic analysis of the chips, one representative chip of each colour (silver, golden, and blue/purple), indicated by arrows in the bar chart in Figure 7, was selected for a more detailed microstructural examination following the methodology shown in Figure 3. The main microstructural observations are presented in Figure 8. The analysis reveals clear differences in the chip back surface among the different conditions and oxide colours. Noticeable microstructural alterations are observed in the golden and blue/purple chips (Figure 8b and c) compared to the silver-coloured chips (Figure 8a).

According to Sun and Guo [26], the localized temperature rise taking place at the tool–chip interface at the secondary shear zone (where the back surface is formed), leads to a reduction in the volume fraction of the $\beta$-phase and a severe elongation of the remaining grains. The thickness of this phase-transformed layer increases with cutting speed, correlating with the higher thermal loads generated. However, this thermal influence is highly localized; the bulk chip microstructure remains largely unaffected due to the rapid quenching effect of the surrounding environment.

Regarding the bulk chip morphology, adiabatic shear bands were observed under all tested conditions. In the golden and blue/purple chips—indicative of higher cutting temperatures—the saw-tooth frequency was lower, with more pronounced serrations, than in the silver chips. This increased chip segmentation is associated with larger fluctuations in cutting forces [27] and temperature [28], reflecting greater machining instability, as the shear bands accommodate higher localized strain [23]. These effects may ultimately degrade the machined surface topography [29].

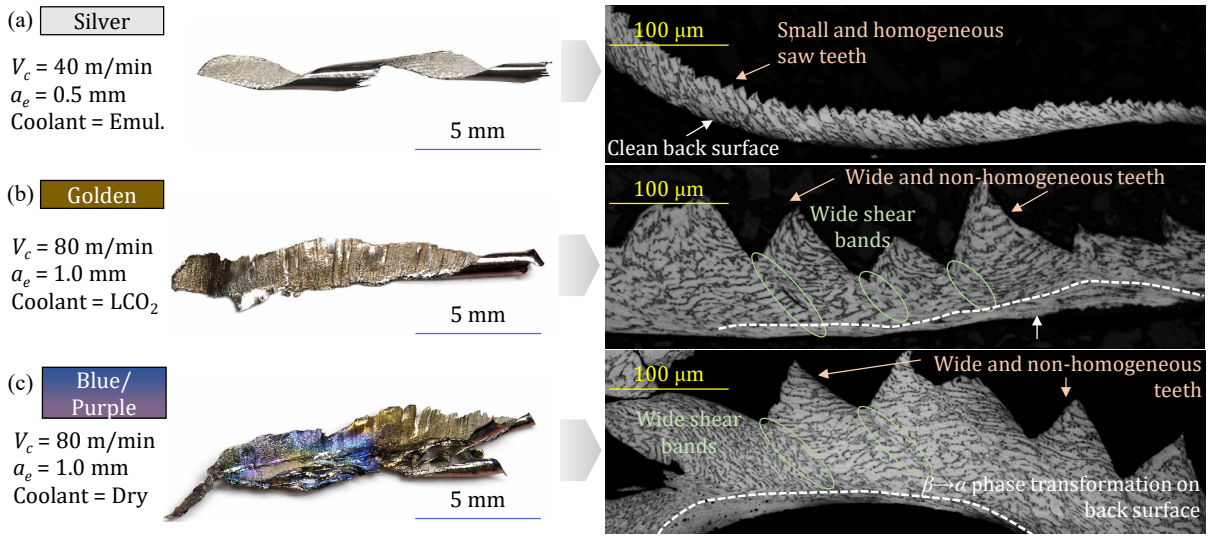


**Fig. 8.** Microstructure analysis of chips with different oxide colours: (a) Silver; (b) Golden; (c) Blue/Purple.

## Conclusions

This study investigated milling parameters and cooling strategies to produce low-oxidation Ti6Al4V chips suitable for solid-state recycling (SSR), providing insights into process windows for circular material flows. The main findings are:

- Flood emulsion cooling proved to be the most robust strategy, consistently producing silver coloured, low-oxidation chips across all tested cutting speeds and radial depths of cut. It acts as a dual mechanism: lubricating the cutting zone to reduce heat generation at the source (reflected in lower tangential forces) and creating a physical barrier against atmospheric oxygen. This combination enables higher material removal rates while effectively preventing chip oxidation.

- $LCO_2$ cooling, a clean oil-free alternative, showed a limited process window. It effectively suppressed oxidation at lower material removal rates ($a_e$ = 0.5 mm). However, under higher thermal loads ($a_e$ = 1.0 mm and elevated cutting speeds), the cooling capacity of $LCO_2$ was exceeded, leading to "blue" and "purple" oxidized chips similar to those from dry cutting.
- A trade-off between productivity and circularity is evident. $LCO_2$ cooling produces clean, low-oxide chips at the cost of reduced material removal rates, whereas emulsion cooling supports higher productivity but may require subsequent cleaning prior to SSR.
- Machining conditions that reduce friction, as achieved with emulsion cooling, are more effective in limiting oxidation than approaches that focus solely on lowering cutting temperature, such as $LCO_2$ cooling, indicating that forces serve as a reliable proxy for assessing potential feedstock quality.
- Chip microstructure and shear behaviour are strongly influenced by localized temperatures, with chips exhibiting golden or blue/purple oxides showing back-surface alterations, reduced $\beta$-phase content, elongated grains, and pronounced adiabatic shear bands, which indicate higher temperatures and greater machining instability compared with silver chips.

Future work will focus on the detailed chemical and microstructural characterisation of the oil and oxide layers on the chips, including quantifying the emulsion-derived oil film and measuring oxide thickness and composition. The aim is to correlate these layer properties with the interfacial bonding and performance of consolidated SSR components.

## Acknowledgements

The authors would like to express their great appreciation to REVIR (KK-2025-0114) and DIGIAERO (ZL-2024/00651) projects for their support to carry out this research.

## References

[1] A. Buesa, L. Pedauga, P. Piñero, J.M. Rueda-Cantuche, B. Baldassarre, Can circularity in titanium metal improve EU strategic autonomy? Scenario modelling with heterogeneous data, JRC Working Papers in Economics and Finance, No. 2024/6, European Commission, 2024. https://hdl.handle.net/10419/311091

[2] K. Georgitzikis, E. D'Elia, U Eynard, Titanium Metal: Impact assessment for supply security, European Commission JRC, JRC129594, 2022. https://publications.jrc.ec.europa.eu/repository/handle/JRC129594

[3] A. Georgitzikis, K. Jakimów, M. Piñero, P. Maury, T. Latunussa, L. Pedauga, V. Samokhalov, B. Baldassarre, F. Mathieux, J.M. Rueda-Cantuche, D. Stijepic, A. Reys, A. Bilous, P. Notom, L. Tercero, Titanium metal in the EU: Strategic relevance and circularity potential, European Union, 2025.

[4] Airbus, Global Market Forecast 2025-2044, Available at: https://www.airbus.com/en/products-services/commercial-aircraft/global-market-forecast. (accessed 23 January 2026).

[5] R. M'Saoubi, D. Axinte, S. L. Soo, C. Nobel, H. Attia, G. Kappmeyer, S. Engin, W. M. Sim, High performance cutting of advanced aerospace alloys and composite materials, CIRP Ann., 64 (2): 557–580, 2015. https://doi.org/10.1016/j.cirp.2015.05.002

[6] D. K. Chouhan, M. Komarasamy, S. B. Taysom, N. R. Overman, N. L. Canfield, T. J. Roosendaal, A. P. Reynolds, S. A. Whalen, Friction-based recycling: An evaluation of friction extrusion for fabricating Ti-6Al-4V wire from machining chip feedstock, Int. J. Adv. Manuf. Technol., 137(5):2519–2528, 2025.

[7] S.A. Smythe, B.M. Thomas, M.Jackson, Recycling of titanium alloy powders and swarf through continuous extrusion (Conform) into affordable wire for additive manufacturing, Metals, 10(6): 843, 2020.

[8] B. Denkena, M. A. Dittrich, V. Suntharakumaran, S. Kettelmann, Recycling of Ti–6Al–4V chips for closed-loop manufacturing, CIRP Ann., 73(1):73–76, 2024. https://doi.org/10.1016/j.cirp.2024.04.046

[9] B. Denkena, T. Grove, P. Helmecke, Recycling of Ti-6Al-4V chips: Influence of the machining process on the chip quality, Proc. 13th World Conf. Titan., 291–298, 2016.

[10] S. Patankar, Y. Thye Kwang, T. Ming Jen, Alpha casing and superplastic behavior of Ti-6Al-4V, J. Mater. Process. Technol., 112(1):24–28, 2001. https://doi.org/10.1016/S0924-0136(00)00849-9

[11] L. Wegewitz, W. Maus-Friedrichs, R. Gustus, H. J. Maier, S. Herbst, Oxygen-free production—From vision to application, Adv. Eng. Mater., 25(12):2201819, 2023. https://doi.org/10.1002/adem.202201819

[12] B. Denkena, B. Bergmann, F. Schaper, Investigation of chip formation of Ti–6Al–4V in oxygen-free atmosphere, Int. J. Adv. Manuf. Technol., 124(10):3601–3613, 2023.

[13] B. Denkena, B. Bergmann, N. Hansen, R. Lang, Influence of an oxygen-free atmosphere on process forces and workpiece quality during surface grinding of Ti-6Al-4V, Lubricants, 11(8):347, 2023.

[14] B. Bergmann, F. Schaper, Study of the effect of oxygen level on tool wear in machining Ti-6Al-4V, CIRP Ann., 73(1):41–44, 2024. https://doi.org/10.1016/j.cirp.2024.04.048

[15] B. Bergmann, B. Denkena, F. Schaper, Thermomechanical tool loading and chip formation in oxygen-free titanium cutting, CIRP J. Manuf. Sci. Technol., 45:253–259, 2023.

[16] V. Prasanthan, B. Denkena, B. Bergmann, Influence of XHV-adequate atmosphere on surface integrity, Prod. Eng., 17(1):57–63, 2023. https://doi.org/10.1007/s11740-022-01143-w

[17] I. Rodriguez, P. J. Arrazola, M. Cuesta, F. Pušavec, Hole quality improvement in CFRP/Ti6Al4V stacks using optimised flow rates for LCO2 and MQL sustainable cooling/lubrication, Compos. Struct.,329, 2024. https://doi.org/10.1016/j.compstruct.2023.117687

[18] I. Rodriguez, P. J. Arrazola, M. Mori, G. Ortiz-de-Zarate, A. Madariaga, A cradle-to-cradle life cycle assessment framework linking machining parameters, tool life and part durability, J. Manuf. Syst., 84:207–222, 2026. https://doi.org/10.1016/j.jmsy.2025.11.021

[19] O. M. P. Neto, A. Calleja-Ochoa, I. Ayesta, A. Rodríguez, H. González-Barrio, A cleaner milling process replacing emulsion coolant by cryogenic CO2, Int. J. Precis. Eng. Manuf. Green Technol., 11(1):21–32, 2024. https://doi.org/10.1007/s40684-023-00530-7

[20] Z. Keren, T. Shuai, Z. Yuzhe, H. Junli, Z. Nailu, Oxidation characteristics of Ti-6Al-4V machining scraps and their influence on microstructure and fracture behavior in recycled alloys, Mater. Des., 254:114137, 2025. https://doi.org/10.1016/j.matdes.2025.114137

[21] F. Estupinán-López, C. Orquiz-Muela, C. Gaona-Tiburcio, J. Cabral-Miramontes, R. G. Bautista-Margulis, Oxidation kinetics of Ti-6Al-4V alloys by conventional and electron beam additive manufacturing, Materials, 16(3):1187, 2023. https://doi.org/10.3390/ma16031187

[22] G. Ortiz-de-Zarate, A. Madariaga, P. J. Arrazola, T. H. Childs, A novel methodology to characterize tool-chip contact in metal cutting using partially restricted contact length tools, CIRP Ann., 70(1):61–64, 2021. https://doi.org/10.1016/j.cirp.2021.03.002

[23] G. Sutter, G. List, Very high speed cutting of Ti-6Al-4V titanium alloy—Change in morphology and mechanism of chip formation, Int. J. Mach. Tools Manuf., 66:37–43, 2013.

[24] F. Pušavec, L. Sterle, M. Kalin, D. Mallipeddi, P. Krajnik, Tribology of solid-lubricated liquid carbon dioxide assisted machining, CIRP Ann., 69(1):69–72, 2020. https://doi.org/10.1016/j.cirp.2020.04.033

[25] F. Pušavec, D. Grguraš, M. Koch, P. Krajnik, Cooling capability of liquid nitrogen and carbon dioxide in cryogenic milling, CIRP Ann., 68(1):73–76, 2019. https://doi.org/10.1016/j.cirp.2019.03.016

[26] J. Sun, Y. B. Guo, A new multi-view approach to characterize 3D chip morphology and properties in end milling titanium Ti–6Al–4V, Int. J. Mach. Tools Manuf., 48(12–13):1486–1494, 2008.

[27] A. Sela, G. Ortiz-de-Zarate, D. Soler, G. Germain, P. Aristimuño, P. J. Arrazola, Measurement of plastic strain and plastic strain rate during orthogonal cutting for Ti-6Al-4V, Int. J. Mech. Sci., 198:106397, 2021. https://doi.org/10.1016/j.ijmecsci.2021.106397

[28] A. Sela, D. Soler, G. Ortiz-de-Zarate, G. Germain, F. Ducobu, P. J. Arrazola, Inverse identification of the ductile failure law for Ti6Al4V based on orthogonal cutting experimental outcomes, Metals, 11(8):1154, 2021. https://doi.org/10.3390/met11081154

[29] G. Ortiz-de-Zarate, A. Sela, D. Soriano, D. Soler, P. Aristimuño, P. J. Arrazola, Influence of chip segmentation of Ti64 on the topography of the machined surface, AIP Conf. Proc., 2113 (1): 080022, 2019.

The publication of this article was funded by the Mondragon Goi Eskola Politeknikoa, J.M.A. S.Coop